이학석사 학위논문

Implementation of Scanning Tunneling Microscope /Atomic Force Microscope utilizing Length Extension Resonator

길이확장 공진기를 이용한
주사형 터널링/원자간력 현미경의 구현

2014년 2월

서울대학교 대학원

물리천문학부

오 명 철

Implementation of Scanning Tunneling Microscope /Atomic Force Microscope utilizing Length Extension Resonator

길이확장 공진기를 이용한 주사형 터널링/원자간력 현미경의 구현

지도교수 국 양

이 논문을 이학석사 학위논문으로 제출함

2014년 2월

서울대학교 대학원

물리천문학부

오명철

오명철의 이학석사 학위논문을 인준함

2014년 2월

위 원 장 _____ 차국린 _____ (인)

부위원장 _____ 국 양 _____ (인)

위 원 _____ 이진호 _____ (인)

Abstract

Atomic structure of materials can be resolved with scanning probe microscopy. Atomic Force Microscope (AFM) has been used to observe the geometric structure of microscopic sized sample, i.e. biological specimen, chemical compounds. Meanwhile, Scanning Tunneling Microscope (STM) is widely used to study the electronic structure of conducting materials. However, AFM cannot investigate the electronic structures, and STM forbid non-conducting materials. AFM integrated STM surmounts these shortcomings, by operating different functions of them at the same time.

For AFM integrated STM, quartz resonator based AFM can be adopted to implement the system. In this thesis, the Length Extension Resonator (LER), a tiny quartz resonator, is mounted on STM head with an Ir-tip for non-contact mode AFM. Having high stiffness, LER can prevent 'jump to contact' effect, and acquire high resolution.

For frequency modulation mode AFM operation, Phase Locked Loop (PLL) is used to detect frequency variations. Also, to avoid interference from parasitic capacitances and amplify tiny output signal of LER effectively, home-built low temperature pre-amplifier was fabricated.

Keywords : LER, Length Extension Resonator, STM, AFM, Low temperature preamplifier

Student Number : 2012-20371

List of Contents

1. Introduction

More than thirty years after its invention by G. Binnig and H. Rohrer Scanning Tunneling Microscope (STM) [1] has been used in a wide range of research area, and proven itself a useful instrument to investigate diverse conducting materials. By resolving the Si(111) 7X7 reconstruction structure [2], STM opened a new era in the observing nano-sized structures. It stimulates many enthusiastic scientists to conduct various experiments in surface science of condensed matter [3-6], and inspires creative ones to develop new scheme of instruments, such as Atomic Force Microscope. It is suitable system so far to measure not only atomic scale topographic feature but also local density of states of electrons. In addition to observe electronic topography and spectroscopy, STM can manipulate several atoms [7] to position specific location on the surface, and this can results distinctive quantum mechanical behaviors.

Atomic Force Microscope (AFM) invented by G. Binning, C. F. Quate, and C. Gerber in 1986 [8] is also one of the most influent scientific instruments as a successor of STM. Unlike STM, whose operation capability is only limited to conducting solids, AFM is suitable for both conducting and non-conducting materials; even if the material is not a solid. It' s because AFM measures Van-der-Waals force between a tip and a sample using cantilever and optical alignment, while STM reads the tunneling current flowing surface of conducting material. Although it only shows topography, this availability for any

kinds of samples, AFM is more widely used in various areas of research rather than STM.

It seems difficult to combine these two different kinds of microscope, because their conventional operation schemes, such as AFM using optical alignments and STM using walker in limited space, are likely to incompatible in UHV and low temperature environment. In spite of such limitations, a piezoelectric quartz resonator based AFM made it possible to break this invisible barrier between them. A piezoelectric quartz resonator abbreviated as quartz resonator, a tiny oscillator, is small enough to mount on limited space of STM head and operates properly in UHV and low temperature environment. Also, its self-sensing property helps excluding complicated optical alignments that incur adverse impacts on UHV environment.

In this thesis, I used 640kHz Length Extension Resonator (LER), one of the quartz resonators, as a cantilever to implant AFM in STM, due to its large quality factor (Q-factor) and high stiffness. With low temperature pre-amplifier, it is anticipated that LER based STM/AFM can uncovers surface features such as geometry of real space and electronic structure simultaneously in high resolution with less limitations of specimens; both insulator and conductor are available. Also, we can expect another possibility of application through this physical instrument, such as atomic resolution AFM with CO-terminated tip [9].

2. Theoretical Backgrounds

2.1. Working principles of STM and AFM

The advent of Scanning Tunneling Microscope(STM) and Atomic Force Microscope(AFM) in 1980s has given impetus to researching varied surface features of materials. Although AFM's operation mechanism resembles that of STM in that STM is a precursor of AFM, they are hardly correlated with each other in measuring physical characteristics: STM reads tunneling currents between a tip and a sample by controlling the vacuum tunneling gap, ATM detects atomic force between them by manipulating deflection of cantilever. These differences make them combine together arduously. Recently, some techniques are developed for implementing AFM integrated STM; piezoelectric quartz resonator based AFM. Its own property facilitates merging two different physical instruments. We should scrutinize about STM and AFM operations individually, before understanding mechanisms about LER based STM/AFM.

2.1.1. Principles of Scanning Tunneling Microscope

Scanning Tunneling Microscope provides topography and spectroscopy by measuring tunneling. When a sharp tip made of conducting materials move around over a conducting sample surface, the tunneling current between them flows, and it

depends on distance z from the apex of the tip to the uppermost surface of the sample. The tunneling probability p is given by.

$$p \propto |\Psi(0)|^2 e^{-2\kappa z}$$

,where $\kappa = \sqrt{2m(U-E)}/\hbar$ is the decay constant and $|\Psi(0)|^2$ is the probability of an electron at the tip position. From Bardeen's approximation [10] to separate electron's state of tip from that of sample, Tersoff and Hann derived simple form to describe tunneling current [11,12]. With the tunneling matrix M that involves dependence on the overlapping of wave-functions between tip and simple, tunneling probability at certain distance is given by,

$$p = \frac{2\pi}{\hbar}\left|M_{\mu\nu}\right|^2 \delta(E_\nu - E_\mu)$$

under the Fermi golden rule, where ν denotes for the sample, μ for the tip, and

$$M_{\mu\nu} = \frac{\hbar^2}{2m}\int d\vec{S}\cdot(\Psi_\mu^* \nabla\Psi_\nu - \Psi_\nu \nabla\Psi_\mu^*).$$

After more arduous tasks using above formalisms, tunneling current can be written as

$$I = \frac{2\pi e^2 V}{\hbar}\sum_{\mu,\nu}\left|M_{\mu\nu}\right|^2 \delta(E_\mu - E_\nu)\delta(E_\nu - E_F)$$

$$= 32\pi^3 e^2 V \hbar^{-1} \phi^2 D_t(E_F) R^2 \kappa^{-4} e^{2\kappa R} \sum_\nu |\Psi_\nu(\vec{r_t})|^2\, \delta\left(E_\nu - E_\mu\right).$$

This equation includes the local density of states (LDOS) of sample at the position $\vec{r_t}$ term, which is $\sum_\nu |\Psi_\nu(\vec{r_t})|^2\, \delta\left(E_\nu - E_\mu\right) \equiv \rho_S(\vec{r_t}, E_F)$. Assuming that the tunneling matrix and the LDOS of the tip are constant, differential tunneling conductance at the specific location is proportional to LDOS at the given voltage,

such as

$$\frac{dI}{dV} \propto \rho_S(E_F - eV).$$

Thus, so called scanning tunneling spectroscopy which visualizes LDOS is the imaging the spectrum of differential tunneling conductance at the given position by sweeping bias voltage.

On the other hand, topography is mapping the intensity of tunneling current, on the ground that tunneling current is exponentially decreases when the tip becomes more distant from the sample. A topographic image can be obtained by two methods; constant height method and constant current method [13]. In the constant height method, the height of a tip is fixed, and STM records the tunneling current flowing between them. By imaging the distance calculated from current−height relation with recorded current, topographic image can be acquired. However, if the set position of tip is lower than sample surface, the tip may be damaged by collision with sample.

In the constant current, distance between tip and sample is determined from current feedback. STM keeps the flows of tunneling current constant by fixing distance with tip and sample. This distance can be controlled with a z−feedback piezoelectric transducer and the z−feedback information at each point is recorded to draw a topographic image. This method doesn' t need burdensome height calculations and prevents tip−sample collision.

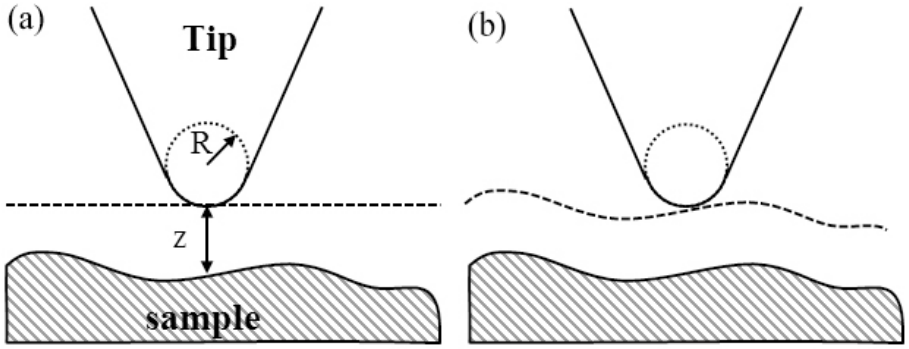

Figure 1. Schematic of picture of STM tip and sample surface with distance z and local radius R. (a) constant height mode, (b) constant current mode.

2.1.2. Principles of non-contact mode AFM

Atomic Force Microscope visualizes geometry of sample surface by using three different method of detecting atomic forces between a tip and a sample: contact mode, non-contact mode, tapping mode. In the contact mode [14] of the cantilever type AFM, Van-der-Waals force is measured by deflection of a cantilever, which is usually monitored by an optical lever and a segmented photodiode. Furthermore, a proportional integral differential (PID)-feedback controller is employed to retain the deflection of a cantilever, by the feedback controller manipulate the piezoelectric material attached to cantilever to move along normal axis to the sample plane in order to keep set point of bending. Thus the geometric image can be acquired by tracking normal axis movement of the piezoelectric material. The reason this operation is referred to as "contact mode" is that this scheme uses repulsive mode.

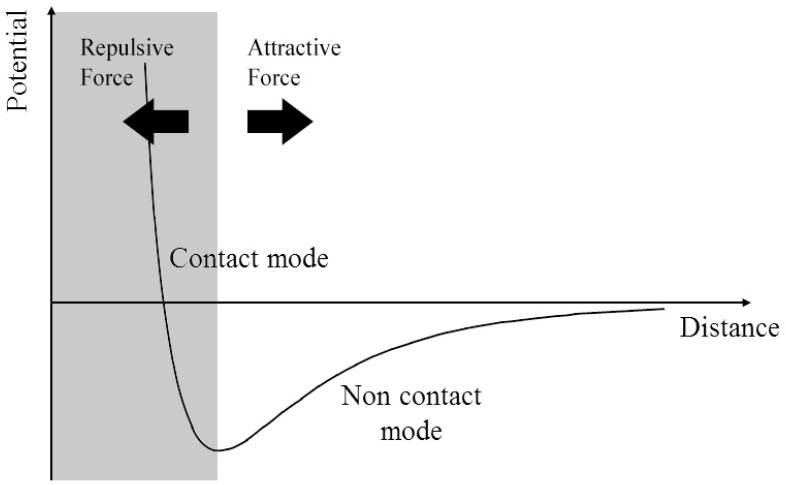

Figure 2. Van-der-Waals potential vs. distance relation

On the other hand, another operation mechanism so called non-contact mode, is somewhat different with aforementioned one. Unlike contact mode AFM, non-contact mode AFM [15] [16] uses attraction force to measure atomic force between a tip and a sample. The tip of non-contact mode AFM acts on at farther distance than contact mode regime, so the tip doesn't touch the sample. Therefore, the interacting force between the tip and a sample is about 10 times weaker than contact-mode, and this weak interaction impedes to perceive the deflection of the cantilever. To detect this small evidence of deflection, frequency modulation technique is used.

In frequency modulation, cantilever itself is regarded as a natural resonator which has its own resonance frequency. This cantilever always oscillates itself at specific frequency; in many case this frequency correspond to resonance frequency. The photodiode monitors its frequency, amplitude and phase from

reflected laser beam. Non-contact mode AFM (NC-AFM) can be represented as simplified model (simple harmonic oscillating model), as shown Figure 1.

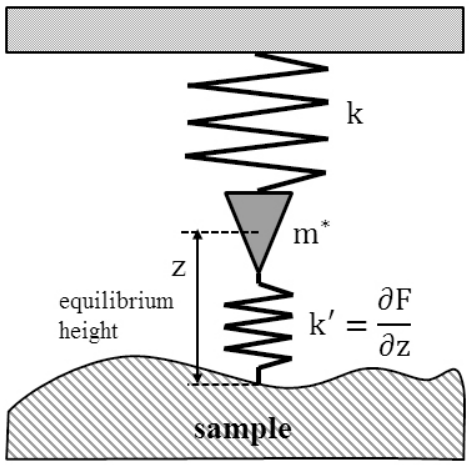

Figure 3. Simple harmonic oscillating model of non-contact mode AFM

Carefully looking around this model, the resonance of the AFM cantilever can be calculated by

$$f_0 = \frac{1}{2\pi}\sqrt{\frac{k_{\text{eff}}}{m^*}}$$

,where m^* is effective mass of the cantilever and k_{eff} is effective spring constant given by [17]

$$k_{\text{eff}} = k + \frac{\partial F}{\partial z}$$

,where k is force constant of lever and $\partial F/\partial z$ force gradient acting on lever due to interaction between a tip and a sample. When the tip approaches to the sample surface appropriately, attraction force shifts cantilever' s resonance curve as shown Figure 4.

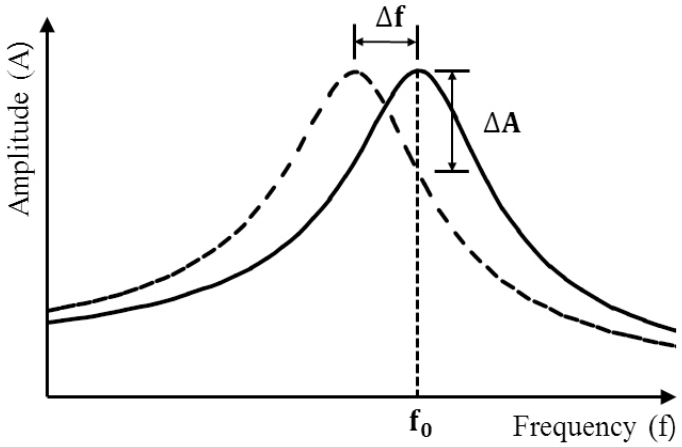

Figure 4. Resonance curves. Solid curve represents resonance without interaction, and dashed curve represent it with interaction

If this change in amplitude of resonance curve at fixed frequency is used for imaging topography and feedback loop, the AFM is said to be run in amplitude modulation (AM) mode. AM mode is simple to design and implement at the expense of some disadvantages, such as vulnerability to the external noises and limitation of scan speed. These drawbacks can be solved by using frequency modulation (FM) mode. In FM mode, AFM tracks resonance peak where the amplitude is maximized by employing phase locked loop technique. Since scanning speed doesn't depends on Q factor and frequency variation is relatively strong against external noise interferences in FM mode, it clears up several problems occurred in AM mode and provides better performance. By using FM mode, we can use high-Q-proof cantilever or resonator which is very important in UHV low temperature environment where Q-factor of cantilever increases.

2.2. Theoretical background of LER

AFM was developed as a tool that investigates topographic feature of a material's surface. Cantilever, a structure interacting with atoms on a target material, is typically used to implement an AFM. However, this method is not suitable for spatially restricted environment such as small head of STM, and requires troublesome optical alignment in a UHV chamber. Another possible method is to use piezoelectric quartz resonator. It is compact and easy to implement, while showing high performance of AFM, compared with other methods, because of several unique advantages. Being simple in configuration, piezoelectric quartz resonator can easily be utilized in a wide range of applications, e.g. experiments in low temperature. A self-sensing capability due to piezoelectricity facilitates instrumentation without complicated optical alignments which are required in conventional cantilever method. Moreover, quartz resonator has advantages to investigate atomic scale (< nm) in that it oscillates with smaller amplitude (about 10^-2 ~ 1nm, cantilever: about 1nm~100nm) and has a higher stiffness (about 1k~1000kN/m, cantilever: about 1~100N/m). Operation with small oscillation amplitude enables to observe atomic feature, such as molecular bonding or lattice structure. However, for the non-contact AFM (NC-AFM), because the tip approaches closely in order to detect atomic structure, attraction force between tip and a sample becomes larger enough to impede recovering to prevent

snapping (“jump to contact”) [12]. To avoid this, stiffness of the resonator should be high enough to overcome attractive force, and quartz resonator’s high stiffness makes “jump to contact” effect inconsiderable.

2.2.1. Basics of LER sensing

Length Extension Resonator (LER), which is the one of the piezoelectric quartz resonator used AFM [19] [20], has high quality factor and stiffness. Since LER itself has high stiffness about 10~20times as much as conventional tuning fork, which is another piezoelectric quartz resonant, it is more favorable than tuning fork to measure strong atomic forces and to prevent “jump to contact” effect.

A LER consists of two coupled beams and one elongated quartz bar (Figure 5(a)). The centered quartz bar is the only active part of this structure, which oscillates itself when AC voltage is applied to one of its electrodes. An ideal length extension resonator has a nodal axis parallel to the axis of the quartz crystal going the bar [21], and two wires are attached to the each side of resonator’s surface at the nodal axis as show in Figure 5(b). Because of piezoelectricity, it expands or contracts itself in the z-direction when different voltage is applied to opposite side of it, so AC voltage drives it oscillating back and forth. If the frequency of the AC voltage corresponds to the bar’s resonance frequency, its oscillation amplitude reaches maximum and resulting output current due to piezoelectricity can also be maximized. Its resonance frequency

thus can be measured easily by tracing maximum current.

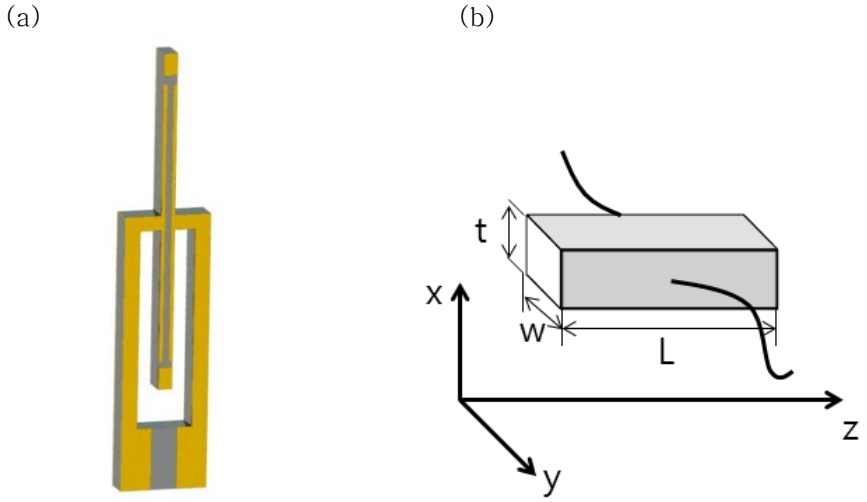

Figure 5. (a) Length extension Resonator (LER), (b) Simplified model of LER

The eigenmode of the resonator is a longitudinal standing wave and its maximal deflection occurs at the end of the bar, thus the length of the bar L corresponds to a multiple of a quarter wavelength $n\lambda/4$. With velocity of sound is $\sqrt{E/\rho}$, where E is Young's modulus and ρ is density, the eigen-frequency is given by,

$$f_0 = \frac{n\sqrt{E/\rho}}{4L}. \ (n = 1,2,3 \ldots)$$

For the typical LER, the coupled beams acting as a suspension hold a resonant quartz bar being referred as tine, and those roots are attached on the center of each side of the tine as shown Figure. 2, so the n value should be 2 or more value. Therefore, the fundamental eigen-frequency that stands

for the resonance frequency is $\sqrt{E/\rho}/2L$. With the longitudinal stiffness k of the tine is given by

$$\mathrm{k} = \frac{Ewt}{L},$$

and the calculated longitudinal stiffness of the LER of this experiment is about 289kN/m.

In frequency modulation atomic force microscopy, the action of force gradients changes the resonant frequency of a force sensor vibrating constant amplitude by a frequency shift $\Delta\mathrm{f} = \mathrm{f} - \mathrm{f}_0$. For the resonator, stiffness k is much stronger than gradient of the tip−sample forces. Therefore, with $\mathrm{f}_0 = \frac{1}{2\pi}\sqrt{\frac{k_{\mathrm{eff}}}{m^*}}$ (m∗ is effective mass, which can be defined in simple harmonic oscillating model of a force sensor), the frequency shift is given by

$$\Delta\mathrm{f} = \frac{\mathrm{f}_0}{2\mathrm{k}}\frac{\partial F}{\partial z}$$

From above equation, frequency shift is proportional to the force gradient. Therefore, relation between tip−sample distance and frequency shift $\Delta\mathrm{f}$ follows force gradient curve as shown Figure 6.

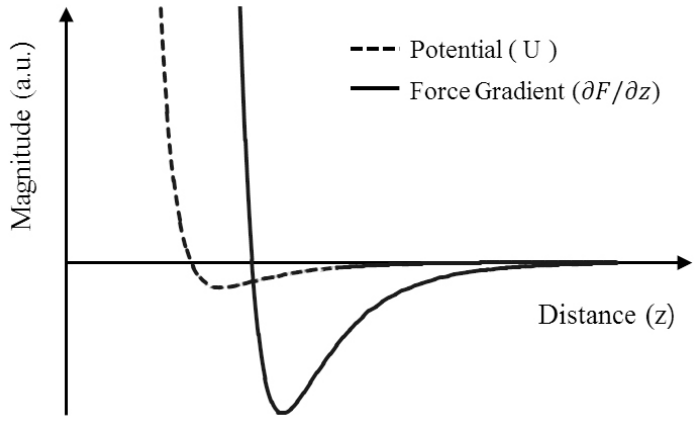

Figure 6. Tip−sample force gradient and potential curve vs. distance

For the reason that LER has high stiffness, tip can approach much closer to the sample than conventional cantilevers and tuning forks. Hence, the operating range of LER can be near the contact regime, and frequency shift dramatically changes. AFM scanning image is acquired by depicting this frequency shift, or visualize Z feedback which holds frequency shift constant.

2.2.2. Signal noises of LER

There are several AFM applications using length extension resonator, but they don’ t have better performance, in spite of large Q−factor and good sensitivity. In order to choose good resonator for the experiment, it is necessary to consider noise sources.

Thermal noise

Thermal noise is the fundamental noise source disturbing frequency detection. Large Q-factor and low stiffness improve signal-to-noise ratio (SNR) by reducing thermal noise. The thermal noise density in force gradient measurement is given by [22]

$$\delta n_{th} = \sqrt{\frac{4kk_BT}{\pi A^2 f_0 Q}}.$$

From this equation, thermal noise density ($\mathrm{V}/\sqrt{\mathrm{Hz}}$) is small in large Q and small k in that thermal noise is proportional to $\sqrt{\mathrm{k}/\mathrm{f_0 Q}}$. The 1MHz LER typically used in AFM application has Q=15000 and k = 540000 at room temperature (300K), so its thermal noise density is about $900\,\mu\mathrm{N/m}\cdot\sqrt{\mathrm{Hz}}$ at 300K, when A=100pm.

In this thesis, 640kHz LER with Q=28300 and k=289000 at 300K is utilized. According to the equation above, its thermal noise density is calculated about $600\,\mu\mathrm{N/m}\cdot\sqrt{\mathrm{Hz}}$; it is 33% lower than 1MHz LER.

Oscillator noise

In Frequency Modulation AFM, there is another contribution of noise sources. In FM-AFM, driving input of the resonator is determined by Phase Locked Loop (PLL) outputs as a feedback loop. If the feedback signal' s amplitude is fed to PLL with noisy input signal, phase detector will generate incorrect output which hampers the PLL to generate exact frequency what is

originally expected. With this noise contribution proportional to n_q, noise in force gradient is given by [22]

$$\delta n_{osc} = \sqrt{2}\frac{kn_q}{QA}.$$

For the 1MHz LER, noise density calculated from this equation is $k_{osc} = 4.6\text{mN/m} \cdot \sqrt{\text{Hz}}$. Likewise, for the 640kHz LER, noise density is $\delta k_{osc} = 2.4\text{mN/m} \cdot \sqrt{\text{Hz}}$.

Thermal frequency drift noise

Eigen-frequency of the resonator can drift by the thermal variation, This drift contribute to noise sources, and this magnitude depends on the drift frequency rate r and measurement period τ . The noise density of thermal drift is given by [22]

$$\delta n_{drift} = \frac{2kr\sqrt{\tau}}{f_0 \pi f_{mod}},$$

where f_{mod} is modulation frequency. It is simply proportional to k/f_0, which is 0.54 for the 1MHz LER and 0.42 for the 640kHz LER.

From above noise consideration, 640kHz LER has better noise performance than 1MHz LER. Consequently, its high stiffness and good noise performance, 640kHz LER is adopted for implementation of AFM, and it is anticipated to show better resolution than conventional 1MHz LER.

3. Instrumentation

3.1. UHV LT STM head

For scanning tunneling current with measuring atomic force, established STM system was modified. Since UHV Low Temperature STM designed to top-loading sample type ensures thermal stability at low temperature around 4K and isolates external mechanical oscillation well, its head was amended to mount LER tip holder. LER tip holder involves three electrodes to operate as an AFM and STM head. To isolate other electrical component, mounting stage is made of ceramic material with three sockets for inserting the electrodes. As shown Figure 7, ceramic tube attached on piezoelectric tube in STM walk unit, and LER stage mounted on the tube.

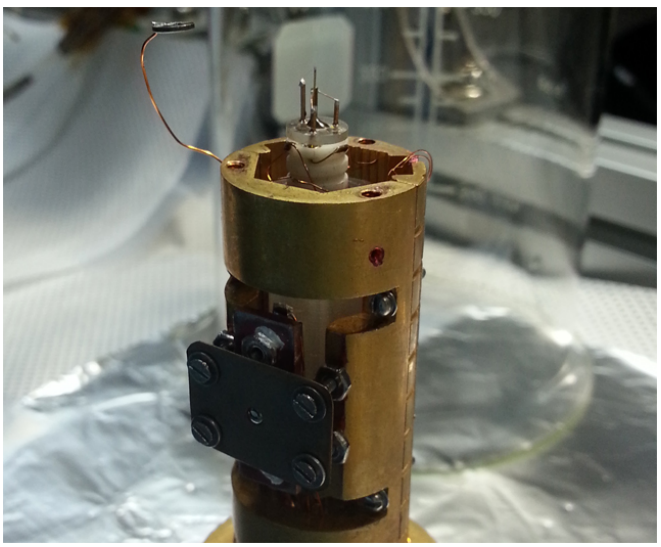

Figure 7. LER stage mounted on STM head

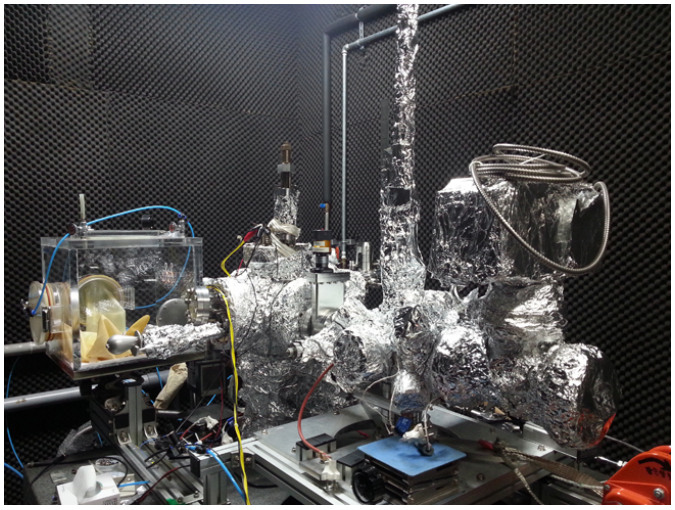

Figure 8. UHV LT STM system

3.2. LER with Ir-tip

3.2.1. Assembling of LER stage

Metal tip connected length extension resonator (LER) is an integral part of this system. To implement LER to UHV STM system, the stage in which STM tip inserts should be modified appropriately. There are three electrodes attached through holes of a sapphire round plate; one for STM, other two for AFM. Sapphire plate is good electrical insulator and thermal conductor, so it forestalls interference of each electrode and cools down the LER and the tip. The LER stands on the center of the plate by epoxying insulating epoxy which has high hardness, due to stiffness.

Three electrodes are made of 0.5mm CuBe wire due to its resilience which fixes tip holder to STM head and provides

sufficient electrical contact. Copper wires attached to two electrodes and then adhere to each arms of LER, thus they can deliver input AC signal to LER and convey its output to pre-amplifier.

A gold wire dia.12.5μm connected to the longest electrode prepared for reading tunneling current passed through metal tip attached to the end of center rod of LER. Since it is inert and strong, the Ir tip is used for scanning tunneling current. This hardness of the Ir tip facilitates to measure strong force between a tip and a sample without change in its shape. Resonance frequency itself is crucial factor for AFM imaging in that it affects Q factor and frequency shift which are related with sensitivity and noises. Thus, the tip which adhere to end of the tine should small in size, because mass of the tip determines resonance frequency roughly proportional to $f_0 \propto 1/\sqrt{m}$, where m is total mass of the tine and the tip. The tip is made of Ir wire dia.125μm. The pre-etching process, similar to typical iridium tip etching process but it only reduces diameter of the wire to 10um~20um, makes the wire thinner. I etched the wire with 30V AC current by using 50% $CaCl_2$ solution as an etchant and graphite as a cathode. After the pre-etching process, this attenuated wire put on the end of the tine of LER, with conductive epoxy.

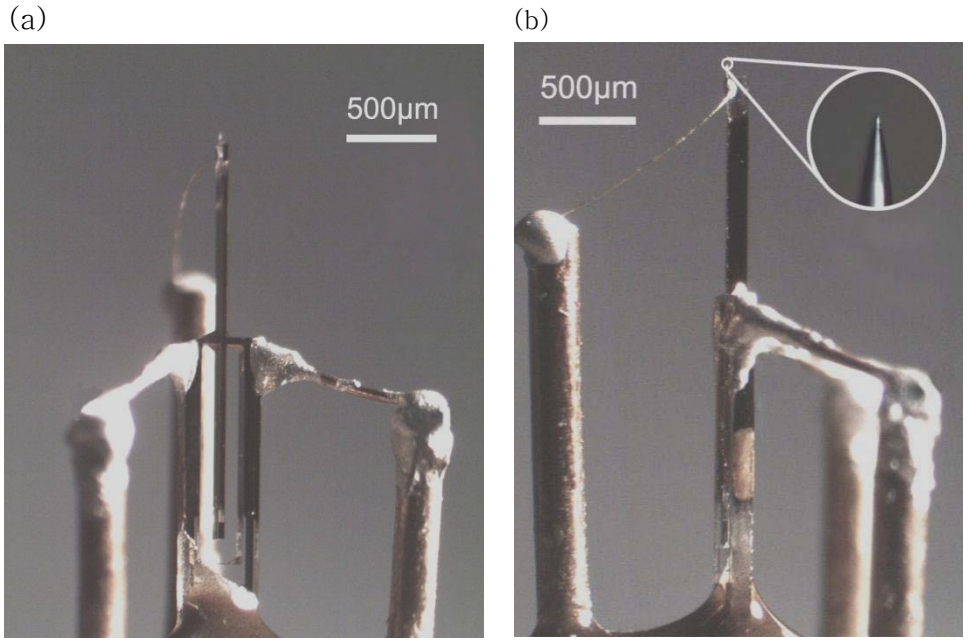

Figure 9. LER stands on the stage. (a) Front, (b) Side image

To fix the tip to the tine of LER, home-built tip assembling stage was used, because the tine of LER is too tiny and fragile to deal with. This assemble stage consist of motorized micrometer stage, epoxy heater, and two arms for holding tip and smearing epoxy as shown Figure 11. In this stage, I attached also the 12.5um to the end of the tine and the electrically connected it with the tip by conductive epoxy. After curing the epoxy tip was etched again through the post-etching process, which makes the tip sharp, and then DI water treatment is conducted to wash contaminations.

In AFM, it is important to sharpening the tip to ensure good quality result. The apex of AFM tip should be sub-micrometer order in size to improve resolution. In order to make the apex of the tip sharp enough, the tip was sharpened by Focused Ion Beam (FIB).

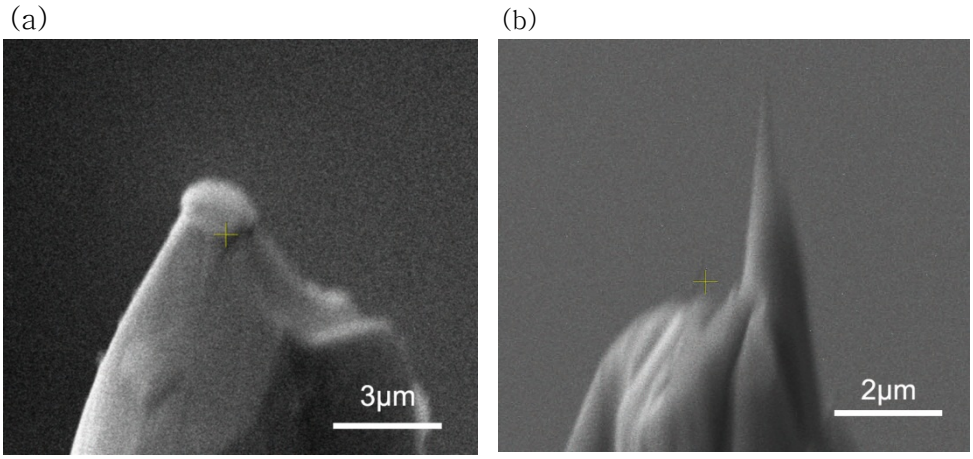

Figure 10. End of the Ir-tip (a) before and (b) after Focused Ion Beam milling process

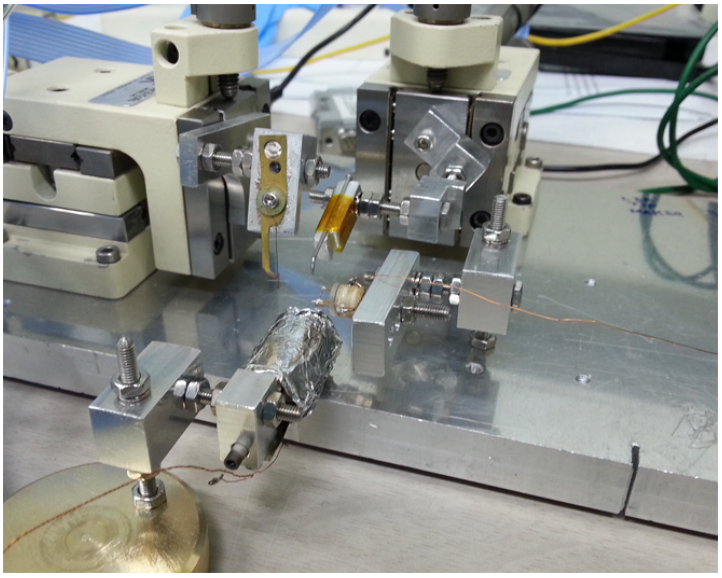

Figure 11. Tip assembling stage

3.2.2. Operation test

To test LER operation with Ir-tip, resonance peak detection was conducted by using low temperature pre-amplifier and

PLL. As shown Figure 12. , resonance curve was obtained, and resonance frequency is about 626841Hz. The resonance frequency is lower than that of LER without tip (640kHz), because additional mass decreases resonance frequency according to the formula aforementioned. This shift of resonance causes lowering Q-factor value, so that width of resonance curve has been broadened.

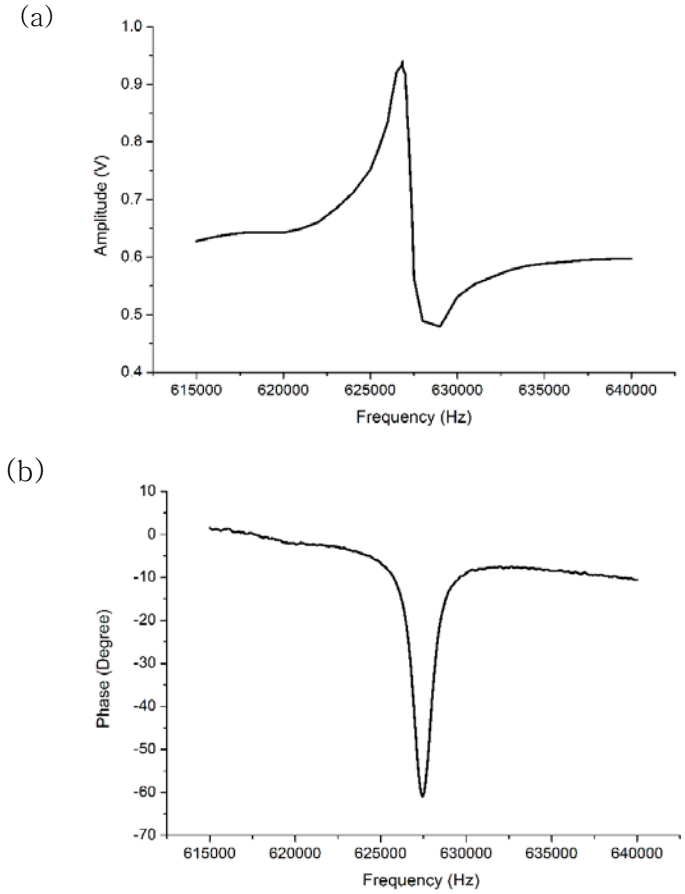

Figure 12. (a) Amplitude and (b) phase response of the LER with It-tip

3.3. Low temperature pre-amplifier system

3.3.1. Design and implementation

To measure the resonance frequency signal, current output of the length extension resonator (LER) should be amplified, because output current signal is tiny in magnitude (10~100nA). Likewise STM, the quartz resonator based AFM needs trans-impedance amplifier (current to voltage amplifier) in order to enlarge signal size enough to measure.

The LER is simply considered as a capacitor varying its capacitance as frequency changes. Since the capacitance of the LER can be relatively smaller than the parasitic one, its output signal can be interfered readily to parasitic capacitance, Also capacitances from the signal transfer wire weakens output signal current. Therefore, to avoid unexpected capacitances generated from the system itself, it is desired to shorten the distance between the resonator and amplifier as much as possible. If the amplifier located near the head, which mounts LER, it should be cooled down when the head is in low temperature. In low-temperature around 4K, there exist a problem that semiconductor device such as op-amp doesn't work well due to decreased electron mobility. To overcome this problem, we separate a mirror stage in an op-amp from the op-amp itself, and put the stage on the parts in low temperature.

The low temperature pre-amplifier is comprised of two

parts: low temperature (LT) mirror stage and post-amplifying stage. The LT mirror stage acts as a simple differential amplifier with drain resistors. It consists of coupled transistors and one resistor.

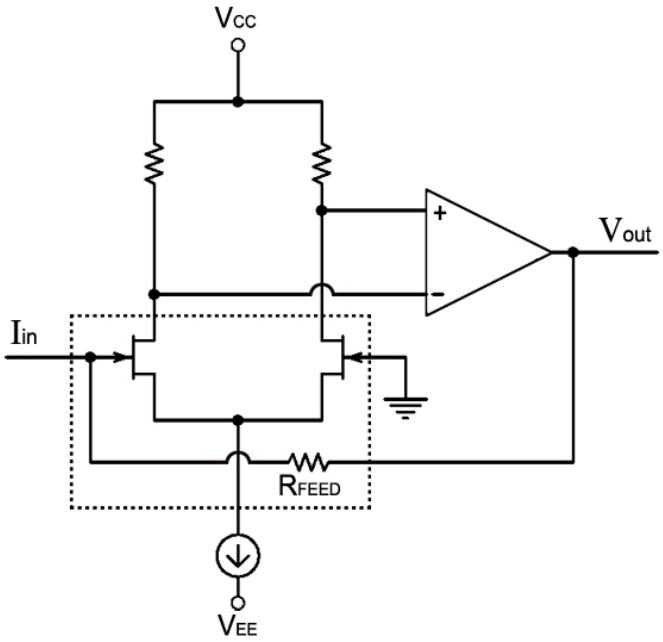

Figure 13. Circuit diagram of the pre-amplifier. The part in the dot-lined box is the LT mirror stage and the other part is the post-amplifying stage.

The transistors soldered on the LT mirror stage are GaAs based MESFETs, which have high mobility than Si-based MOSFETs, so the pre-amplifier is able to operate in high-frequency range. The resistor in the LT mirror stage shown figure above is a feed-back resistance, that transforms current signal to voltage one with amplifying the magnitude of the signal.

The signal which the transistors amplify enters to the op-amp at the post-amplifying stage, and the signal is amplified

much more than before. Since open-loop gain of the transistors limits output bandwidth and current-voltage gain, additional op-amp should follows after the stage in order to attain high gain-bandwidth product. Simply, the preamplifier except feedback resistor serves as an op-amp. Thus, we can easily regard whole preamplifier as an inverting amplifier.

In the post-amplifying stage OP847 is used, in that it has high gain-bandwidth product (8.2G) with low noise, so we could ensure 50M current-to-voltage gain and ~1.5MHz bandwidth with 50MΩ feedback resistor. Generally magnitude of the output signal current is 10~100nA in operating range, these gain and bandwidth are enough to measure LER output.

(a) (b)

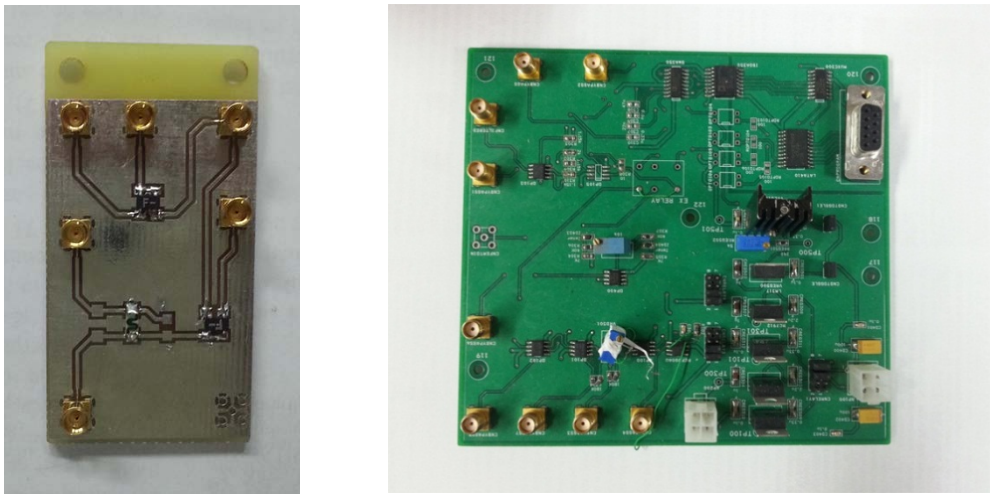

Figure 14. (a) LT mirror stage and (b) Post amplifying stage

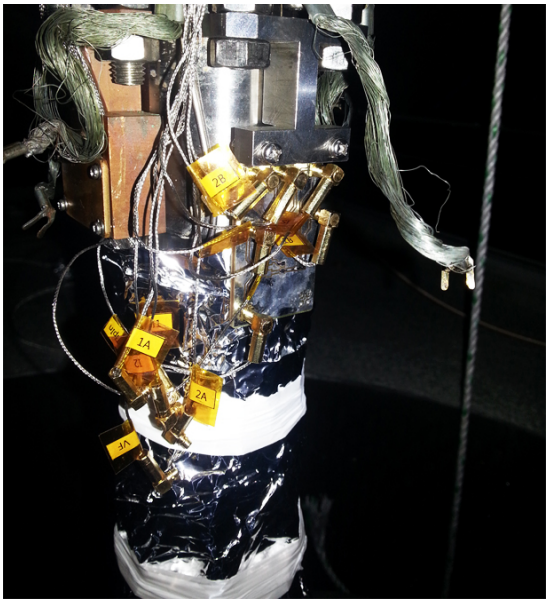

Figure 15. Low temperature mirror stage mounted on the outside of the chamber near the STM head

3.3.2. Operation test at low temperature

To prove operating the pre-amplifier at low temperature, cryogenic dewar was modified and exploited as a test bed. Top cover of the dewar involves 12 electrodes divided into two connectors apart from each other because of averting electrical interferences. The end of the prolonged bar connected with the cover holds LT mirror stage circuit. In order to prevent electric short, this mirror circuit was cooled down indirectly through infused exchange gas He whose temperature falls down near the inside wall of outside LHe chamber.

Operation test was conducted with 30nA-700kHz sinusoidal wave input and 5MΩ feedback resistor. As shown Figure 17., pre-amplifier worked well without meaningful change in shape

and amplitude in low temperature range. Therefore, this pre-amplifier is suitable for low temperature AFM experiment.

(a) (b)

Figure 16. (a) Operation Testing Dewar and (b) inside rod structure

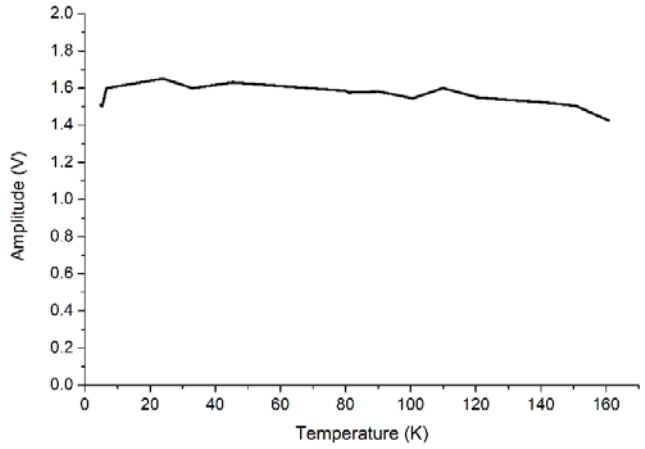

Figure 17. Output response of low temperature pre-amplifier vs. temperature

3.4. Phase Locked Loop

To track resonance frequency in FM-AFM, PLL FM detector is utilized in this thesis. PLL FM detector [23] is equipment whose reference signal is generated to follow input signal $\pi/2$ phase behind. It consists of three main elements: Phase Shifter, Phase Comparator (PC) and Voltage-Controlled Oscillator (VCO). VCO is an oscillator controlled by voltage. It generates a sinusoidal wave and varies its output frequency proportional to input DC voltage. PC compares phase of two input signals -a reference signal and a LER signal - and produces output DC voltage proportional to the phase difference between them. Phase shifter adjust input signal's phase for proper operating condition. Near the resonance frequency, since phase changes dramatically as frequency varies, we should adjust phase of resonance frequency to set point for feedback loop.

The FM-detection process is simple. The output signal of LER passed through phase shifter in proper operating condition enters PC inputs. Then, PC compares input signal of LER i.e. reference signal with output signal of phase shifter. When force gradient between tip and sample shifts resonance frequency and phase of LER, PC detects its difference, and then produces DC voltage to VCO. VCO, then adjust input frequency to keep phase difference between two PC input signals 90 degree. Hence, the phase of output signal of LER keeps constant so that it always vibrates at its resonance frequency. By monitoring reference signal frequency, we can track resonance frequency

shift of LER.

Amplitude Gain Controller (AGC) is a crucial element for FM mode AFM. Since output amplitude depends on input frequency, AGC automatically adjusts gain to keep output amplitude constant so that LER vibrates with constant amplitude. As shown Figure 18., output signal amplitude converts to DC voltage by RMs to DC rectifier. This DC output forwards to AGC , and AGC controls driving signal.

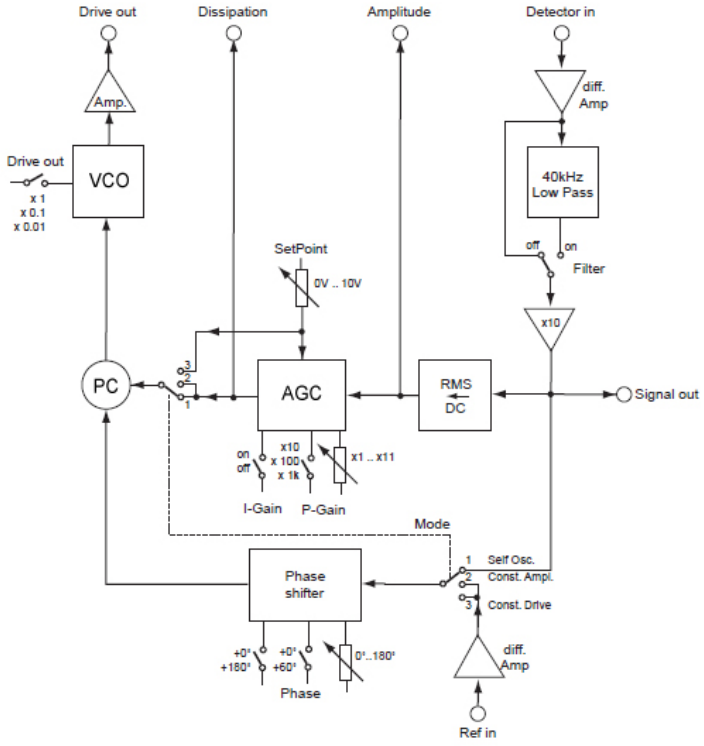

Figure 18. Block diagram of PLL with AGC

4. Summary

A UHV low temperature atomic force microscope integrated scanning tunneling microscope was developed using a 640kHz length extension type quartz resonator. To measure tunneling current, FIB treated Ir-tip which was electrically connected with an electrode through 10μm gold wire was attached to the end of LER.

With a self-sensing characteristic of quartz resonator, small sized AFM was implemented on small-sized STM head without complicated optical alignments. The LER's high stiffness and large Q-factor facilitates to investigate atomic scale feature, and it has better noise performance than conventional 1MHz LER.

Low temperature pre-amplifier was also developed to amplify small output current signal of LER using high-mobility GaAs transistors, which is able to operate at 4K, so that 50M current-voltage gain can be established within 1MHz bandwidth.

Reference

[1] G. Binnig, H. Rohrer, C. Gerber and E. Welbel, *Phys. Rev. Lett.,* no. 49, p. 57, 1982.

[2] G. Binnig, H. Rohrer, C. Gerber and E. Weibel, *Phys. Rev. Lett.,* no. 50, p. 120, 1983.

[3] O. Pietzsch, A. Kubetzka, D. Haude, M. Bode and R. Wiesendanger, *Rev. Sci. Instrum.,* no. 71, p. 424, 2000.

[4] H. P. Rust, M. Doering, J. I. Pascual, T. P. Pearl and P. S. Weiss, *Rev. Sci. Instrum,* no. 72, p. 4393, 2001.

[5] Y. J. Song, A. F. Otte, V. Shvarts, Z. Zhao, Y. Kuk, S. R. Blankenship, A. Band, F. M. Hess and J. A. Stroscio, *Rev. Sci. Instrum.,* no. 81, p. 121101, 2010.

[6] L. Petersen, M. Schunack, B. Schaefer, T. R. Linderoth, P. B. Rasmussen, P. T. Sprunger, E. Laegsgaard, I. Stensgaard and F. Besenbacher, *Rev. Sci. Instrum.,* no. 72, p. 1438, 2001.

[7] M. Crommie, C. P. Lutz and D. M. Eigler, *Science,* no. 262, p. 218, 1993.

[8] G. Binnig, C. F. Quate and C. Gerber, *Phys. Rev. Lett.,* no. 56, p. 930, 1986.

[9] L. Gross, N. Moll, F. Mohn, A. Curioni, G. Meyer, F. Hanke and M. Persson, *Phys. Rev. Lett.,* no. 107, p. 086101, 2011.

[10] J. Bardeen, *Phys. Rev. Lett.,* no. 6, p. 57, 1961.

[11] J. Tersoff and D. Hamann, *Phys. Rev. Lett.,* no. 50, p. 1998, 1983.

[12] J. Tersoff and D. Hamann, *Phys. Rev. B.,* no. 31, p. 805, 1985.

[13] C. J. Chen, Introduction to Scanning Tunneling Microscopy, New York: Oxford University Press, 2003.

[14] Y. Martin and H. K. Wickramasinghe, *Appl. Phys. Lett.,* no. 50, p. 1455, 1995.

[15] B. Gasser, A. Mench, H. Brune and K. Kern, *Rev. Sci. Instrum.,* no. 67, p. 1925, 1996.

[16] A. Kikukawa, S. Hosaka and R. Imura, *Appl. Phys. Lett.,* no. 66, p. 3510, 1995.

[17] T. R. Albrecht, P. Grutter, D. Horne and D. Rugar, *J. Appl. Phys.,* no. 69, p. 668, 1991.

[18] F. J. Giessibl, H. Bielefeldt, S. Hembacher and J. Mannhart, *Appl. Surf. Sci.,* no. 140, p. 352, 1999.

[19] T. An, T. Nishio, T. Eguchi, K. Akiyama and Y. Hasegawa, *Appl. Phys. Lett.,* no. 87, p. 133114, 2005.

[20] T. An, T. Nishio, T. Eguchi, M. Ono, A. Nomura, K. Akiyama and Y. Hasegawa, *Rev. Sci. Instrum.,* no. 79, p. 033703, 2008.

[21] R. J. Dinger, *Freq. Control Symposium*, Neuchâtel, 1981.

[22] F. J. Giessibl, F. Pielmeier, T. Eguchi, T. An and Y. Hasegawa, *Phys. Rev. B,* vol. 84, p. 125409, 2011.

[23] *EasyPLL FM sensor controller and detector,* AG, Switzerland: Nanosurf.

[24] F. J. Giessibl, *Appl. Phys. Lett.,* vol. 78, p. 123, 2001.

[25] F. J. Giessibl and H. Bielefeldt, *Phy. Rev. B,* vol. 61, p. 9968, 2000.

초 록

물질의 원자적 구조는 주사탐침현미경을 통해서 분석할 수 있다. 그 중 원자간력현미경은 생물학적 시료, 화합물등 마이크로사이즈의 작은 샘플표면의 기하학적 구조를 관찰하는데 사용되어 왔다. 한편, 주사형 터널링 현미경은 전도체 물질의 전자적 성질을 연구하는데 널리 쓰이고 있다. 하지만 주사형터널링현미경은 부도체물질을 연구할 수 없고, 원자간력현미경은 물질의 전자적구조를 알 수 없다는 단점이 있다. 원자간력현미경이 통합된 형태의 주사형 터널링 현미경은 동시에 이들의 다른 기능을 이용하게 함으로써 이런 단점들을 극복할 수 있다.

원자간력현미경이 통합된 주사형 터널링 현미경을 구현하기 위하여, 수정 진동자 기반의 원자간력현미경이 이번 시스템에 채택이 되었다. 이 논문에서는 작은 수정진동자인 길이확장공진기가 이리듐 팁을 단 상태로 주사형 터널링 현미경의 헤드부분에 장착되었다. 길이확장 공진기는 높은 강성을 가지고 있기에 높은 해상도를 얻을 수 있고, 접점뛰기 효과를 방지할 수 있다.

주파수 변조모드의 원자간력현미경을 이용하기 위해서, 위상고정루프를 이용하여 주파수의 변화를 측정하였고, 직접 설계 제작한 저온 프리앰프를 이용하여, 기생 커패시턴스의 간섭을 효과적으로 줄이면서 길이확장공진기의 작은 출력신호를 증폭할 수 있었다.

주요어: 주사형 터널링 현미경, 길이 확장 공진기, 원자 간력 현미경
학번: 2012-20371